DOI: 10.4274/TurkJOrthod.2025.2025.61

TURKISH JOURNAL OF
ORTHODONTICS

Original Article

Orbital Compartment Stress Responses Related to Rapid Maxillary Expansion: A Finite Element Analysis

Aybüke Ensarioğlu, Arzu Arı Demirkaya

İstanbul Okan University Faculty of Dentistry, Department of Orthodontics, İstanbul, Türkiye

Cite this article as: Ensarioğlu A, Arı Demirkaya A. Orbital compartment stress responses related to rapid maxillary expansion: a finite element analysis. *Turk J Orthod.* 2025; 38(3): 161-169

Main Points

- Stress, particularly around the orbital compartment, increases with bone ossification; however, this can be reduced by using a hybrid device.
- Significant stresses occur at the superior orbital fissure and optic foramen, through which the oculomotor nerve and the optic nerve pass.
- Increased ossification reduces displacement but elevates Von Mises stresses, thereby increasing the risk of neurovascular compression.

ABSTRACT

Objective: This study aimed to use finite element analysis to evaluate the effects of acrylic HYRAX and hybrid HYRAX devices in the treatment of rapid maxillary expansion (RME), particularly on the orbital compartments.

Methods: In the present study, a craniofacial model was developed utilizing computed tomography data obtained from the visible human project. A total of four distinct models were generated by designating the sutures in the adult variation as closed and those in the non-adult variation as open while incorporating both expansion devices into the model. Both acrylic and hybrid device models were subjected to expansion forces of 0.25 mm and 5 mm, yielding eight distinct scenarios for comprehensive analysis.

Results: Significant stress and displacement were observed, particularly around the orbital compartments in all scenarios. Displacement decreased with increased sutural ossification and the resulting stresses demonstrated elevation. In adult models, the hybrid device generated reduced stress, especially around the orbital compartments.

Conclusion: Based on these findings, it is proposed that the orbital compartments may serve as a clinically relevant site for measuring the increased intracranial pressure during RME treatment. To prevent possible side effects, RME should be performed at an early age, and if ossification is suspected to be increased, bone-supported expansion devices are recommended.

Keywords: Hybrid HYRAX, orbital compartment stress, FEA, RME

INTRODUCTION

Transversal maxillary deficiency is among the most common skeletal problems in the craniofacial region.[1] The concept of separating the maxillary halves through rapid maxillary expansion (RME) was first introduced by E.H. Angell in 1860. Currently, a variety of appliances are used for this purpose, including tooth-supported, tooth-and-tissue-supported, hybrid (tooth-and-bone-borne), and bone-supported appliances. During tooth-supported RME, orthopedic forces of up to 100 N have been reported,[2] with effects transmitted not only to the maxilla but also to adjacent cranial bones through their associated sutures.[3] In animal studies involving rhesus monkeys, increased cellular activity was observed not only in the maxilla but also in the nasal, zygomaticomaxillary, and zygomaticotemporal sutures adjacent to the maxilla.[4] Furthermore, sutural separation has been observed even

Corresponding author: Aybüke Ensarioğlu, MD, **e-mail:** aybukeensarioglu@gmail.com
Received: June 19, 2025 **Accepted:** September 04, 2025 **Publication Date:** September 30, 2025

in the lambdoid and parietal sutures, and spheno-occipital synchondrosis.[5]

Maturation of the midpalatal suture, which progresses with the completion of growth, reduces the potential for transverse expansion.[6] As this maturation increases, the forces generated during RME are increasingly transmitted to surrounding craniofacial structures. One region that may be particularly susceptible to these stresses is the eye-maxillary complex, including the orbital floor, infraorbital rim, and maxillary sinus, where even minor skeletal changes could potentially affect orbital support and surrounding neurovascular pathways. Increased mechanical stress in these areas can lead to deformation of adjacent bones, elevated risk of fracture, and potential damage to critical vascular and nerve structures.[7] Reports have also indicated hemodynamic alterations within the brain during RME,[8] along with clinical observations of orbital volume increases and associated elevations in intracranial pressure (ICP), which may result in symptoms such as headache and diplopia.[9,10]

Given the complexity of these anatomical relationships, direct clinical evaluation of such effects remains challenging. Finite element analysis (FEA), an engineering method designed to calculate stress and deformation in complex structures, provides a reliable approach for evaluating these biomechanical changes. It has become a widely applied tool in biomedical research and is increasingly used in orthodontics to model craniofacial responses under various treatment modalities.[11]

Previous FEA studies have assessed the impact of both conventional tooth-supported (acrylic-coated HYRAX) and tooth-bone-supported (hybrid HYRAX) devices on cranial structures. However, their specific effects on the orbital compartment have not been systematically examined. One of the most accessible and non-invasive methods for evaluating changes in ICP is the measurement of the optic nerve sheath diameter (ONSD).[12]

Because the orbital compartment is closely related anatomically to the maxilla and serves as the most clinically feasible site for noninvasive ICP assessment, evaluating its response to RME is essential for determining whether such measurements accurately reflect pressure changes induced by expansion. Therefore, this study aimed to evaluate the effects of acrylic and hybrid HYRAX devices on stress distribution within the orbital compartment during RME at two distinct stages of midpalatal suture maturation.

METHODS

This study was approved by the Marmara University Faculty of Dentistry Clinical Research Ethics Committee (approval no.: 2022/40, date: 24.02.2022). For the creation of the maxilla and craniofacial bone model, computed tomography (CT) data were selected from the visible human project.[13] Tomography data were reconstructed with a slice thickness of 0.1 mm and were then imported into the 3DSlicer software in DICOM (.dcm) format. CT data in DICOM format were separated according to appropriate Hounsfield unit values (Supplementary Table 1) in 3D Slicer software and converted into a three-dimensional model through a segmentation process. The model was exported in STL format.

The three-dimensional model was imported into the ALTAIR Evolve software, where maxillary cortical and cancellous bone and tooth geometries were modeled. The periodontal ligaments (PDLs) were modeled with optimal thickness with reference to the outer surfaces of the teeth. Perimaxillary sutures were developed using cutting surfaces in ALTAIR Evolve, based on bone models obtained from tomography. Both acrylic and hybrid HYRAX devices were also modeled in the same software. In both devices, a 10 mm HYRAX expansion screw was incorporated (Forestadent Snap Lock Expander, Pforzheim, Germany). The hybrid HYRAX device included two 2x8 mm mini screws, two mini screw sleeves, and extensions to the premolars, which represented a modification adopted to enhance anchorage (Tasarımmed, İstanbul, Türkiye). Mini-screws were placed 2 mm laterally to the midpalatal suture in the region of the third palatal ruga, which has been identified in the literature as the most suitable site for screw placement. This location is also anatomically close to the center of resistance of the nasomaxillary complex.[14]

All models were prepared using material properties defined by their Young's modulus and Poisson's ratio values (Table 1) and placed in the correct coordinates in 3D space (Figure 1). The total number of nodes and elements that the models consist of is given in Table 2. To enable force transfer between models, mesh matching was performed in ALTAIR Hypermesh software.

In this study, a mesh convergence test was conducted to ensure the finite element model's reliability and accuracy, aiming for an error rate below 3% while maintaining computational efficiency. To maintain consistency in comparison, each mesh with element sizes ranging from coarse to fine was generated

Table 1. Poisson's ratio and Young's modulus determining the biomechanical properties of the materials in the study[19]

Materials	Young's modulus (MPa)	Poisson's ratio
Hybrid device and acrylic device	110000	0.3
Tooth	20000	0.3
Cancellous bone	1370	0.3
Cortical bone	13700	0.3
PDL	1.18	0.3
Suture	0.68	0.45

PDL, periodontal ligament.

Table 2. Total node and element numbers of models

	Acrylic device	Hybrid device
Total nodes	530,016	706,614
Total elements	2,065,964	2,827,372

and analyzed under identical loading and boundary conditions. The variation in the evaluation metric was observed through comparing results from successive mesh refinements. The relative error between two consecutive meshes was calculated. The process was repeated until the relative error dropped below the 2-3% threshold. Triangular 2D and tetrahedral 3D meshes were used for their suitability in capturing complex geometries and curved surfaces in bone models. Mesh quality was evaluated for skewness angles over 80° and a minimum element length of 0.001, with necessary refinements applied when either criterion was not met.

Activation forces simulating 0.25 mm, and 5 mm displacement along the X-axis (transverse direction) were applied to both acrylic and hybrid devices across all models (Figure 1). These values correspond clinically to activations of 1/8 turn and 5 turns, respectively. The load was transmitted to the maxilla via the expansion appliance. Distinct analysis scenarios were established for adult and non-adult variations using the same model: adult scenarios were simulated with closed sutures, and non-adult scenarios with open sutures. A total of eight static analyses were solved linearly under the specified loading conditions.

To calculate the stress and strain effects created by the externally applied force on the model, three boundary conditions were applied in this study:

• Boundary condition shown in blue: The models were fixed at the nodes around the foramen magnum by restricting all degrees of freedom to prevent movement in all three axes (Figure 2).

• Boundary condition shown in red: A boundary condition was applied on the X-axis normal, symmetrical with respect to the Y-Z plane (Figure 2).

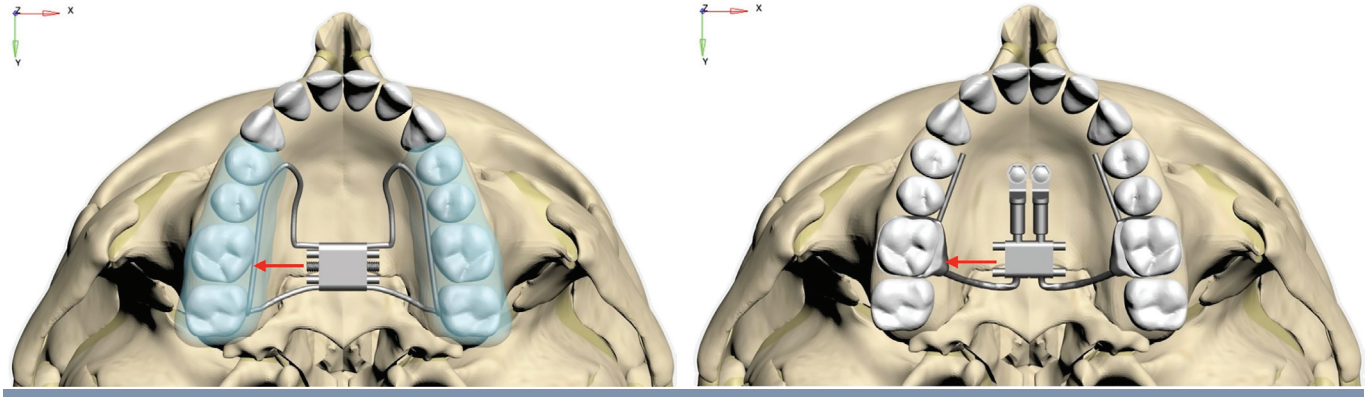

Figure 1. A) Acrylic HYRAX device placed in the correct coordinates in 3D space and activation forces simulated along the X-axis. **B)** Hybrid HYRAX device, including two 2x8 mm mini screws and two sleeves, placed in the correct coordinates in 3D space and activation forces simulated along the X-axis

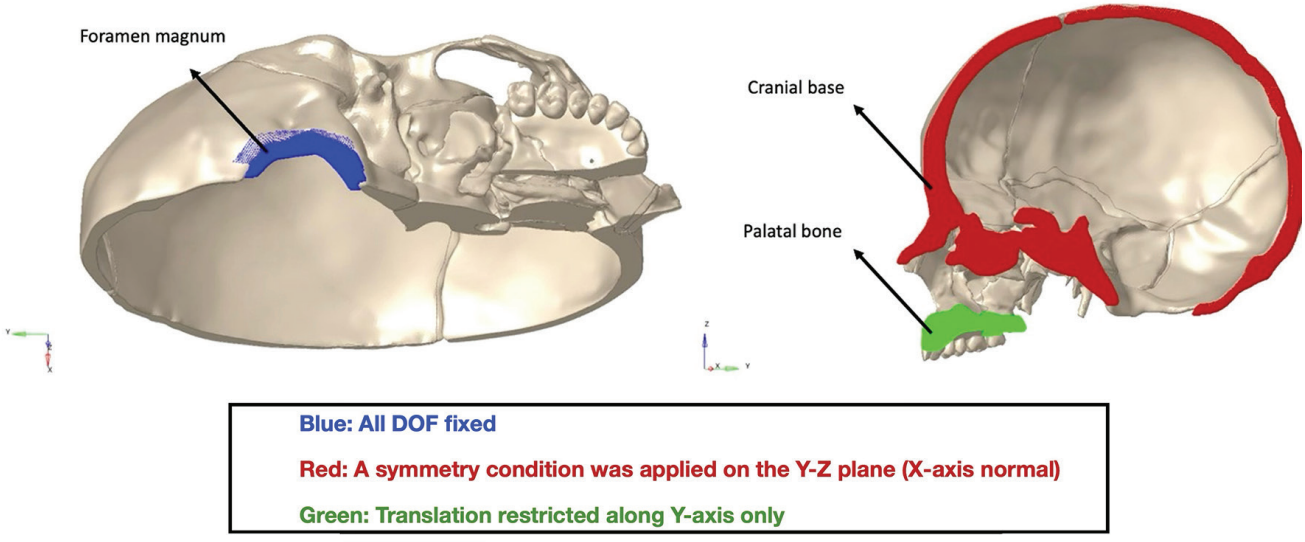

Figure 2. Boundary condition shown in blue: The models were fixed at the nodes around the foramen magnum by restricting all degrees of freedom (DOF) so that the movement in all three axes is prevented, Boundary condition shown in red: The palatal bone was modeled as two unconnected segments separated by the vertical plane of symmetry, permitting unrestricted lateral movement relative to this plane (X-axis normal, symmetrical with respect to the Y-Z plane) , Boundary condition shown in green: All cranial points on the symmetry plane (Y-axis) were constrained from motion perpendicular to it, except for the palatal bone, which remained fully unconstrained

• The boundary condition shown in green is applied to restrict motion in the Y-axis only (Figure 2).

A FREEZE type contact was defined in the bone-suture and bone-PDL-tooth contact areas, based on the assumption that these areas move in full correlation during displacement.

After obtaining the mathematical models, we solved the FEA using Nastran-based ALTAIR Optistruct (2021, Altair Engineering, Inc., Troy, MI, USA) implicit solver.

Through FEA, the 0.25 mm and 5 mm displacement amounts in the models were measured in millimeters (mm), along the X (transversal plane), Y (anteroposterior plane), and Z (vertical plane) axes. Von Mises stress values were calculated in megapascals (MPa=N/mm^2) and presented as color-mapped images. Each color in the obtained images represents a stress range, and the color scale is displayed to the left of each image.

RESULTS

In this study, von Mises stresses resulting from the initial activation of 0.25 mm, and the displacement amounts resulting from a total expansion of 5 mm for both acrylic and hybrid devices in adult and non-adult models were evaluated. Given that the forces generated during RME do not increase cumulatively as screw activation increases, additional investigation into the impact on bone remodeling is necessary. Therefore, von Mises stresses resulting from 5 mm expansion were not evaluated as they do not accurately represent clinical scenarios. The values resulting from a 0.25 mm expansion were also excluded from evaluation due to their negligible amounts.

0.25 mm Activation

When the Von Mises stresses after 0.25 mm expansion in the non-adult models are examined (Figure 3); the highest total craniofacial stress was observed in the acrylic device (18.97 MPa), followed by the hybrid device (10.38 MPa). Stress at the lateral orbital tubercle was also higher in the acrylic device (3.63 MPa) than in the hybrid device (1.88 MPa). While stress in the optic foramen was higher than in the infraorbital foramen with the acrylic device, the stress in the optic foramen was lower with the hybrid device (Table 3).

When the Von Mises stresses after 0.25 mm expansion in the adult models were examined (Figure 4), the total craniofacial stress was once again the highest in the acrylic device (106.68 MPa), followed by the hybrid device (18.58 MPa). Stress in the lateral orbital tubercle was significantly greater in the acrylic device (21.23 MPa) compared to in the hybrid device (3.35 MPa). While stress in the optic foramen was higher than in the infraorbital foramen with the acrylic device, it was lower in the hybrid device (Table 4).

In both devices, stress values were higher in the adult models compared to the non-adult models following 0.25 mm expansion.

5 mm Activation

When the resultant displacements after 5 mm expansion in the non-adult models were examined (Figure 5), total resultant displacement across all craniofacial structures was highest with the acrylic device (40.89 mm), followed by the hybrid device (21.72 mm). The greatest resultant displacement was observed at the zygomaticomaxillary suture (1.86 mm) in the hybrid device, and at the pterygoid hamulus (6.92 mm) in the acrylic device. Total resultant displacement was higher in an acrylic device, particularly in regions surrounding the orbital area. Although the junctional displacements in the optic foramen and superior orbital fissure were similar between devices, they

Table 3. Von Mises stresses (MPa) at 0.25 mm expansion in non-adult models with both devices

	Acrylic	Hybrid
Lateral orbital tubercle	3,6396	1,8885
Zygomaticomaxillary suture	2,7924	1,5132
Optic foramen	0.9088	0.536
Foramen rotundum	0.9083	0.5327
Infraorbital foramen	0.6781	0.5474
Medial pterygoid lamina	0.6102	0.3098
Carotid canal	0.569	0.3498
Foramen ovale	0.3897	0.2156
Superior orbital fissure	0.2166	0.1528
Lateral pterygoid lamina	0.2099	0.1157

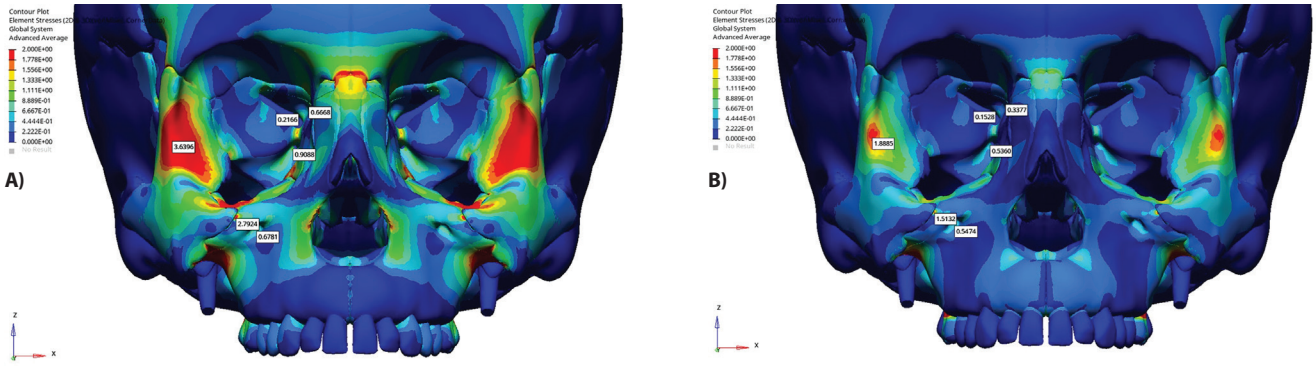

Figure 3. A) Von Mises stresses in the non-adult model given an expansion force of 0.25 mm with Acrylic device. **B)** Von Mises stresses in the non-adult model given an expansion force of 0.25 mm with Hybrid device

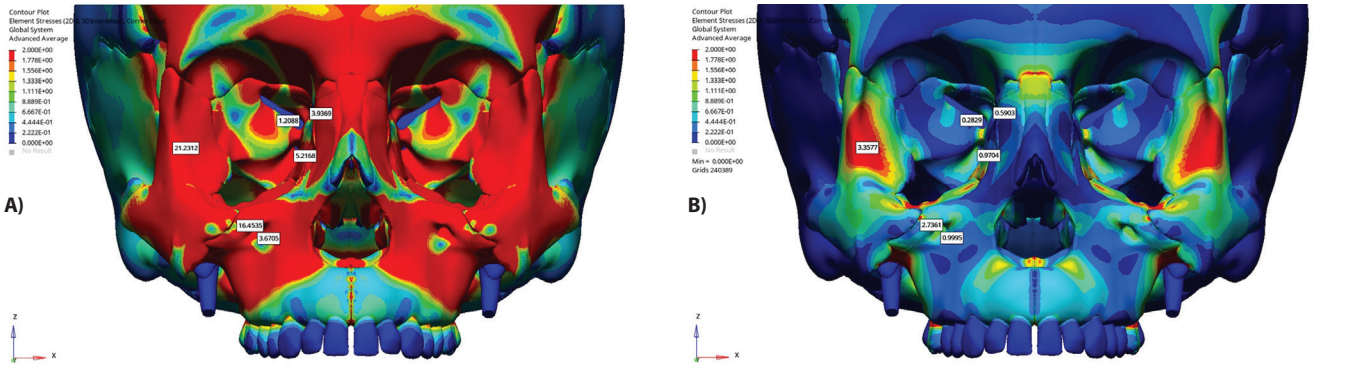

Figure 4. A) Von Mises stresses in the adult model given an expansion force of 0.25 mm with Acrylic device. **B)** Von Mises stresses in the adult model given an expansion force of 0.25 mm with Hybrid device

Table 4. Von Mises stresses (MPa) at 0.25 mm expansion in adult models with both devices

	Acrylic	Hybrid
Lateral orbital tubercle	21,2312	3,3577
Zygomaticomaxillary suture	16,4535	2,7361
Foramen rotundum	5,2291	0.9636
Optic foramen	5,2168	0.9704
Medial pterygoid lamina	3,6964	0.5562
Infraorbital foramen	3,6705	0.9995
Carotid canal	3,2436	0.6455
Foramen ovale	2,2409	0.3876
Lateral pterygoid lamina	1,2159	0.2104
Superior orbital fissure	1,2088	0.2829

was greater with the acrylic device. In the adult models, the resultant displacement at the infraorbital foramen was notably higher with the acrylic device (1.42 mm) compared to the hybrid device (0.43 mm) (Table 6).

In both devices, displacement were higher in the non-adult models compared to the adult models, following 5 mm expansion.

DISCUSSION

Numerous clinical and animal studies have investigated the effects of RME on skeletal and dental tissues.8 In addition, many studies using finite element analysis have been published, examining these effects.[15,16] Published studies consistently report that the effects of RME are not limited to the dentoalveolar region and midpalatal suture but extend to more extensive craniofacial structures through the sutures, potentially impacting critical neurovascular structures.[5] In two case reports, patients were reported to experience symptom resolution after the discontinuation of RME treatment, which they had undergone due to ocular symptoms.[17,18] Since the ocular region is considered the most clinically accessible and non-invasive site for ICP monitoring,[12] the potential effects of RME on this area warrant careful evaluation. The FEA method

Unlike previous FEA studies, this study employed an acrylic and a modified hybrid device, with extensions to the premolars, selected for their ability to produce greater skeletal effects and reduce dental side effects compared to traditional banded tooth-supported HYRAX devices.[15,22,23] This modification was incorporated based on clinical experience, which emphasized the need to enhance anchorage support in the event of miniscrew failure, thereby allowing the appliance to continue functioning as a tooth-supported device if necessary.

In order to standardize all anatomical factors except sutural maturation, a single CT dataset was modeled; the sutures designated as open for non-adult models and closed for adult models, representing two different age groups. Although the timing of midpalatal suture fusion varies significantly among individuals, with some patients retaining an open suture into early adulthood and others showing partial or complete fusion in their mid-teens 6, the general clinical approach is to perform RME as early as possible to reduce the risk of adverse effects, increased resistance, and relapse associated with delayed treatment.[24]

Von Mises Stress Findings

Regardless of whether the sutures were open or closed, the total Von Mises stresses were found to be higher in the acrylic device than in the hybrid device, consistent with findings from previously published studies. It has been demonstrated that because the hybrid device provides expansion force from a location closer to the center of resistance of the maxilla, the resulting stresses do not spread to the deep tissues of the facial skeleton as much as with the acrylic device.[19]

For both devices, the stresses observed in the adult models were higher than those in the non-adult models. This finding supports the understanding that the elasticity of sutures and bones may decrease with increasing age, thereby increasing the risk of complications that may occur during RME treatment in adult patients.[7]

In this study, the highest stress between the sutures was found to occur in the zygomaticomaxillary suture, as reported

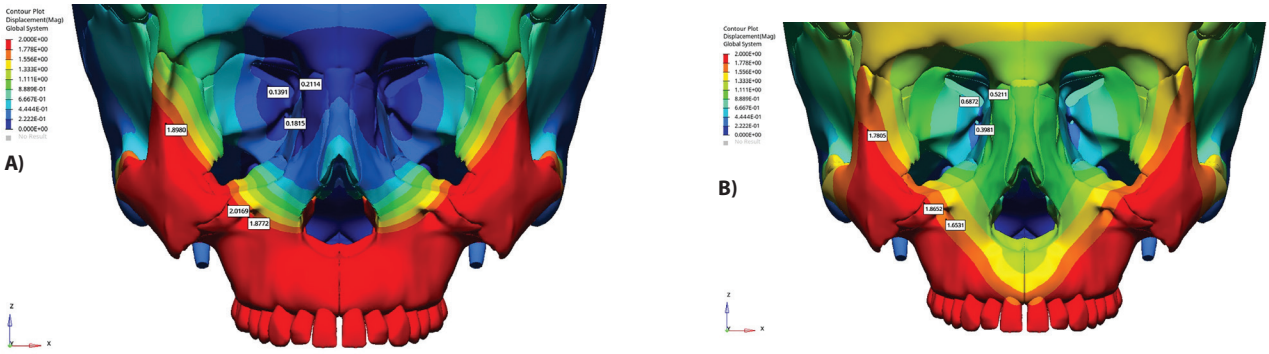

Figure 5. A) Resultant displacement in the non-adult model given 5 mm expansion force with Acrylic device. **B)** Resultant displacement in the non-adult model given 5 mm expansion force with Hybrid device

Table 5. Resultant displacement (mm) at 5 mm expansion in non-adult models with both devices

	Acrylic	Hybrid
Pterygoid hamulus	6,9238	1,7904
Lateral pterygoid lamina	5,138	1,592
Zygomaticomaxillary suture	3,8062	1,8652
Infraorbital foramen	3,523	1,6588
Lateral orbital tubercle	3,0767	1,7805
Medial pterygoid lamina	1,7329	0.4924
Carotid canal	0.6297	0.2047
Optic foramen	0.5478	0.5211
Superior orbital fissure	0.4839	0.4443
Foramen rotundum	0.3992	0.4056
Foramen ovale	0.3216	0.3024

in previous studies.[25] It has also been reported that clinical microcracks may occur due to limited displacement in this region.[26]

It was observed that stresses also occurred in the wings of the sphenoid bone, and pterygoid laminae. There was significant stress at points where important nerves and vascular bundles pass, such as the foramen ovale and foramen rotundum. Particularly in the adult models, the stress that was observed in the foramen rotundum after expansion with the acrylic device (5.22 MPa) was substantially higher than expansion with the hybrid device (0.96 MPa). Holberg and Rudzki-Janson[27] who reported similar results, emphasized that attention should be paid to hypersensitivity in the areas innervated by cranial nerves and temporary ocular movement limitation due to the stresses of RME treatment. They recommended that if rapid expansion treatment is to be performed in adults, surgical assistance should be considered, and the pterygomaxillary junction should be separated prior to expansion.[27]

Around the orbital compartments, the highest stress occurred at the lateral orbital tubercle in all models. In adult models, the acrylic device caused significant stress around the eye (31.32 MPa), whereas, in both adult and non-adult models, the hybrid device was found to cause less stress. Stress around the infraorbital foramen was slightly higher than around the optic foramen in all hybrid models, whereas in all acrylic models, stresses around the optic foramen exceeded those around the infraorbital foramen. However, MacGinnis et al.[19] reported that stresses around the infraorbital foramen were higher than those around the optic foramen in both devices. This discrepancy is thought to be due to the absence of acrylic in the conventional HYRAX device used in their study. Another FEA study yielded similar findings, demonstrating significant stress at the optic foramen and superior orbital fissure. These findings may provide a biomechanical basis for previously reported case studies describing ocular manifestations associated with RME.[7]

The results of this study correlate with the stress findings around the orbital compartments and with previously published case reports of dizziness and tension in the under-eye and cheekbone area during RME treatment.[17]

Resultant Displacement Findings

As in a previous thesis study, the total resultant displacements observed in this study were found to be higher in the acrylic devices under all sutural conditions.[28] The total resultant displacement was found to be higher in the non-adult model than in the adult model for both devices. Although this finding is consistent with previous studies,[7] there is also literature reporting contradictory results.[28] It can be assumed that in adult models, due to increased rigidity of bones and sutures, the amount of displacement caused by expansion forces decreases compared to non-adult models, while the resulting stresses in adult models increase.

In both device models, significant displacements of the lateral and medial pterygoid laminae were observed, consistent with previous studies.[29] Displacements in these regions were consistently greater in the acrylic device across all sutural conditions. Particularly in the adult model, the amount of displacement observed in the hybrid device was substantially lower than that observed in the acrylic device. This finding supports the hypothesis proposed by researchers who have suggested that in adult patients, the use of tooth-bone supported devices, as opposed to tooth-supported devices alone, can reduce complications during RME treatment.[19]

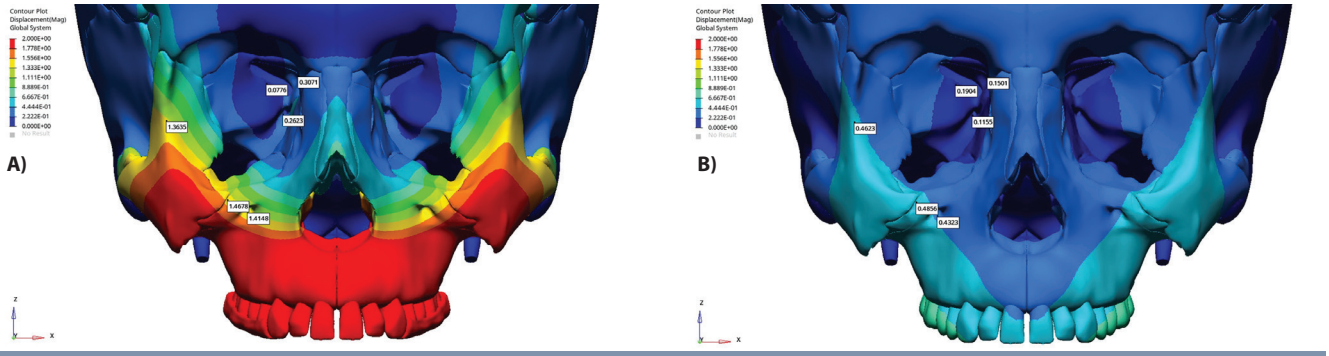

Figure 6. A) Resultant displacement in the adult model given 5 mm expansion force with Acrylic device. **B)** Resultant displacement in the adult model given 5 mm expansion force with Hybrid device

Table 6. Resultant displacement (mm) at 5 mm expansion in adult models with both devices

	Acrylic	Hybrid
Pterygoid hamulus	2,6681	0.4401
Zygomaticomaxillary suture	1,4678	0.4856
Lateral pterygoid lamina	1,9831	0.3985
Infraorbital foramen	1,4281	0.4323
Lateral orbital tubercle	1,3635	0.4623
Medial pterygoid lamina	0.6678	0.1277
Carotid canal	0.3324	0.0631
Optic foramen	0.3071	0.1501
Superior orbital fissure	0.2718	0.1266
Foramen rotundum	0.2567	0.1174
Foramen ovale	0.1239	0.0849

this study found that, particularly when examining the orbital compartment, the total amount of resultant displacement was higher in non-adult models. The acrylic device models caused more displacement around the orbital compartment, with the infraorbital foramen identified as the most significantly affected site. Consistent with previously published studies, significant displacements were also observed in the superior orbital fissure, infraorbital foramen, and optic foramen.[7,28,29] These displacements were notably reduced with the hybrid device, especially in adult models (Figure 6).

It was also observed that in RME-affected craniofacial bones, beyond the maxilla, considerable stress and displacement occurred particularly around the orbital compartment. In a previously published case by Romeo et al.,[17] it was noted that the symptoms, such as double vision and headache, during RME treatment, were caused by the protrusion of the optic nerve head and increased volume in the perioptic subarachnoid space. Additionally, idiopathic intracranial hypertension may develop due to elevated ICP.[17] The most prominent clinical symptoms of IHH include disturbances such as diplopia, headache, and papilledema, which can lead to blindness if not appropriately managed.[30] Therefore, clinical evaluation and reliable measurement of ICP are critical in patients at risk of IHH. Evensen and Eide[12] reported that one of the non-invasive methods for monitoring changes in ICP is ONSD measurement. Based on the findings of this study, the ability to visualize stress and displacement around the orbital compartments during RME, suggests that measuring ICP through the orbital compartment may yield clinically meaningful results.

Study Limitations

The main limitation of this study is the assumption that all anatomical structures, including cortical bone, sutures, and soft tissues, are isotropic and homogeneous, whereas in reality they are anisotropic and heterogeneous. In particular, the PDL exhibits non-linear and viscoelastic behavior, which may significantly influence stress distribution. Additionally, the assumption of bilateral symmetry and the use of a single time point analysis lead to the exclusion of time-dependent force dynamics, potentially limiting clinical applicability. Another limitation is the use of CT data from a single individual, which restricts generalizability, and the assumption of bilateral symmetry with a single time-point analysis, excluding time-dependent force dynamics. Furthermore, individual variability in suture maturation should be acknowledged, Despite these limitations, finite element analysis remains a valuable and comprehensive method for estimating the biomechanical effects of RME. Consequently, it is believed that the findings of this study may help guide future clinical research on the potential impact of RME on ICP.

CONCLUSION

In the expansion treatments performed with both devices, regardless of the suture ossification level, the highest stress was observed at the zygomaticomaxillary suture, rather than the midpalatal suture.

Significant stress and displacement also occurred at the pterygoid laminae of the sphenoid bone, suggesting that hybrid devices should be preferred to reduce neurovascular risks. Stress increased with enhanced sutural ossification, particularly around the orbital compartment, and this stress may be reduced by hybrid devices. During RME, stress were observed in the superior orbital fissure, and optic foramen, which may explain reported ocular symptoms. Based on these findings, it is suggested that the orbital compartments may be used as a clinically relevant site to assess ICP during RME.

As ossification increases, displacement decreases, while stresses increase. To avoid potential adverse effects, early expansion is recommended, and bone-supported devices should be considered in adults.

Ethics

Ethics Committee Approval: This study was approved by the Marmara University Faculty of Dentistry Clinical Research Ethics Committee (approval no.: 2022/40, date: 24.02.2022).

Informed Consent: Informed consent form wasnt taken since its not a clinical trial.

Footnotes

Author Contributions: Surgical and Medical Practices - A.E.; Concept - A.E.; Design - A.E.; Data Collection and/or Processing - A.E.; Analysis and/or Interpretation - A.E.; Literature Search - A.E.; Writing - A.E., A.A.D.

Conflict of Interest: The authors have no conflicts of interest to declare.

Financial Disclosure: This study did not receive any specific grant from funding agencies in the public, commercial, or not-for-profit sectors.

REFERENCES

1. McNamara JA. Maxillary transverse deficiency. *Am J Orthod Dentofacial Orthop*. 2000;117(5):567-570. [CrossRef]
2. Isaacson RJ, Ingram AH. Forces produced by rapid maxillary expansion: II. Forces present during treatment. *Angle Orthod*. 1964;34:261-270. [CrossRef]
3. Seong EH, Choi SH, Kim HJ, Yu HS, Park YC, Lee KJ. Evaluation of the effects of miniscrew incorporation in palatal expanders for young adults using finite element analysis. *Korean J Orthod*. 2018;48(2):81-89. [CrossRef]
4. Starnbach H, Bayne D, Cleall J, Subtelny JD. Facioskeletal and dental changes resulting from rapid maxillary expansion. *Angle Orthod*. 1966;36(2):152-164. [CrossRef]
5. Gardner GE, Kronman JH. Cranioskeletal displacements caused by rapid palatal expansion in the rhesus monkey. *Am J Orthod*. 1971;59(2):146-155. [CrossRef]
6. Angelieri F, Cevidanes LHS, Franchi L, Gonçalves JR, Benavides E, McNamara JA. Midpalatal suture maturation: Classification method for individual assessment before rapid maxillary expansion. *Am J Orthod Dentofacial Orthop*. 2013;144(5):759-769. [CrossRef]
7. Holberg C. Auswirkungen der forcierten Gaumennahterweiterung auf die Schädelbases - Eine FEM-Analyse. *Journal of Orofacial Orthopedics*. 2005;66(1):54-66. [CrossRef]
8. Li Q, Wang W, Zhang Q, Wang L. Changes in CT cerebral blood flow and volume associated with rapid maxillary expansion in a rabbit model. *Angle Orthodontist*. 2012;82(3):418-423. [CrossRef]
9. Sicurezza E, Palazzo G, Leonardi R. Three-dimensional computerized tomographic orbital volume and aperture width evaluation: A study in patients treated with rapid maxillary expansion. *Oral Surg Oral Med Oral Pathol Oral Radiol Endod*. 2011;111(4):503-507. [CrossRef]
10. Lo Giudice A, Rustico L, Ronsivalle V, Nicotra C, Lagravère M, Grippaudo C. Evaluation of the changes of orbital cavity volume and shape after tooth-borne and bone-borne rapid maxillary expansion (RME). *Head Face Med*. 2020;16(1):1-10. [CrossRef]
11. Knop L, Gandini LG, Shintcovsk RL, Gandini MREAS. Scientific use of the finite element method in orthodontics. *Dental Press J Orthod*. 2015;20(2):119-125. [CrossRef]
12. Evensen KB, Eide PK. Measuring intracranial pressure by invasive, less invasive or non-invasive means: Limitations and avenues for improvement. *Fluids Barriers CNS*. 2020;17(1):1-33. [CrossRef]
13. Ackerman MJ. The visible human project. *Proceedings of the IEEE*. 1998;86(3):504-511. [CrossRef]
14. Ludwig B, Baumgaertel S, Zorkun B, et al. Application of a new viscoelastic finite element method model and analysis of miniscrew-supported hybrid hyrax treatment. *Am J Orthod Dentofacial Orthop*. 2013;143(3):426-435. [CrossRef]
15. Oliveira PLE, Soares KEM, De Andrade RM, et al. Stress and displacement of mini-implants and appliance in mini-implant assisted rapid palatal expansion: Analysis by finite element method. *Dental Press J Orthod*. 2021;26(4):1-23. [CrossRef]
16. Sevillano MGC, Kemmoku DT, Noritomi PY, Fernandes LQP, Capelli Junior J, Quintão C. New highlights on effects of rapid palatal expansion on the skull base: a finite element analysis study. *Dental Press J Orthod*. 2021;26(6):e2120162. [CrossRef]
17. Romeo AC, Manti S, Romeo G, et al. Headache and diplopia after rapid maxillary expansion: a clue to underdiagnosed pseudotumor cerebri syndrome? *Journal of Pediatric Neurology*. 2015;13(1):31-34. [CrossRef]
18. Lanigan DT, Mintz SM. Complications of surgically assisted rapid palatal expansion: review of the literature and report of a case. *J Oral Maxillofac Surg*. 2002;60(1):104-110. [CrossRef]
19. MacGinnis M, Chu H, Youssef G, Wu KW, Machado AW, Moon W. The effects of micro-implant assisted rapid palatal expansion (MARPE) on the nasomaxillary complex--a finite element method (FEM) analysis. *Prog Orthod*. 2014;15:52. [CrossRef]
20. Cozzani M, Nucci L, Lupini D, et al. Two different designs of mini-screw assisted maxillary expanders, using FEM to analyse stress distribution in craniofacial structures and anchor teeth. *Int Orthod*. 2022;20(1):100607. [CrossRef]
21. Moaveni S. Finite element analysis theory and application with ANSYS. 5th ed. Prentice-Hall, Inc.; 2003. [CrossRef]
22. Coloccia G, Inchingolo AD, Inchingolo AM, et al. Effectiveness of dental and maxillary transverse changes in tooth-borne, bone-borne, and hybrid palatal expansion through cone-beam tomography: a systematic review of the literature. *Medicina (Kaunas)*. 2021;57(288):1-12. [CrossRef]
23. Gokturk M, Yavan MA. Comparison of the short-term effects of tooth–bone-borne and tooth-borne rapid maxillary expansion in older adolescents. *J Orofac Orthop*. 2024;85(1):43-55. [CrossRef]
24. da Silva Filho OG, Boas MC, Capelozza Filho L. Rapid maxillary expansion in the primary and mixed dentitions: a cephalometric evaluation. *Am J Orthod Dentofacial Orthop*. 1991;100(2):171-179. [CrossRef]
25. Jafari A, Shetty KS, Kumar M. Study of stress distribution and displacement of various craniofacial structures following application of transverse orthopedic forces--a three-dimensional FEM study. *Angle Orthod*. 2003;73(1):12-20. [CrossRef]
26. Ghoneima A, Abdel-Fattah E, Hartsfield J, El-Bedwehi A, Kamel A, Kula K. Effects of rapid maxillary expansion on the cranial and circummaxillary sutures. *Am J Orthod Dentofacial Orthop*. 2011;140(4):510-519. [CrossRef]
27. Holberg C, Rudzki-Janson I. Stresses at the cranial base induced by rapid maxillary expansion. *Angle Orthod*. 2006;76(4):543-550. [CrossRef]
28. Tan E. Evaluation of different ossification stages on maxilla and circumaxillary during rapid maxillary expansion using three different appliance by finite element analysis. Kırıkkale University Institute of Health Sciences; 2014. [CrossRef]

29. Gautam P, Valiathan A, Adhikari R. Stress and displacement patterns in the craniofacial skeleton with rapid maxillary expansion: A finite element method study. *Am J Orthod Dentofacial* Orthop. 2007;132(1):5.e1-5.e11. [CrossRef]

30. Finet P, Delavallée M, Raftopoulos C. Idiopathic intracranial hypertension following deep brain stimulation for Parkinson's disease. *Acta Neurochir (Wien)*. 2015;157(3):443-447. [CrossRef]

Supplementary **Table 1.**

Tissue	Min. HU value	Max. HU value
Cortical bone	662	1988
Cancellous bone	148	661
Tooth	1200	3071